Journal of Molecular Spectroscopy 407 (2025) 111982

Contents lists available at ScienceDirect

Journal of Molecular Spectroscopy

journal homepage: www.elsevier.com/locate/yjmsp

The rotational spectroscopy of dichloromethane ($CH_2^{35}Cl_2$) in the ground state and ν_4 vibrationally excited state from 11 to 750 GHz☆

Manamu Kobayashi [a], Kaori Kobayashi [a,*], Brian J. Esselman [b], R.Claude Woods [b], Robert J. McMahon [b], Satoshi Yamamoto [c], Hiroyuki Ozeki [d]

[a] Department of Physics, University of Toyama, 3190 Gofuku, Toyama 930-8555, Japan
[b] Department of Chemistry, University of Wisconsin-Madison, 1101 University Avenue, Madison, WI 53706, USA
[c] The Graduate University for Advanced Studies (SOKENDAI), Shonan Village, Hayama, Kanagawa 240-0193, Japan
[d] Department of Environmental Science, Faculty of Science, Toho University, 2-2-1 Miyama, Funabashi 274-8510, Japan

ARTICLE INFO

Keywords:
Dichloromethane
Methylene chloride
CH_2Cl_2
Rotational spectroscopy
Hyperfine structure

ABSTRACT

The rotational spectrum of dichloromethane (methylene chloride, CH_2Cl_2) was measured with near-continuous frequency coverage from 29 to 750 GHz with 50 kHz resolution, with additional transitions around 11 GHz with 20 kHz resolution. The rest frequencies of transitions for both the vibrational ground state and first fundamental ν_4 are observed, measured, and least-squares fit. Transitions for both of these vibrational states are modeled with partial octic, distorted rotor A- and S-reduced Hamiltonians in the I^r representation with nuclear quadrupole coupling. Computed spectroscopic constants at the B3LYP/6–311+G(2d,p) level are compared to their corresponding experimental values. The partition function of dichloromethane is updated.

1. Introduction

Dichloromethane (methylene chloride, CH_2Cl_2, Fig. 1) is a frequently used organic solvent with a relatively low boiling point. Chloromethanes are of interest in atmospheric chemistry because of their impact on stratospheric ozone depletion and climate change. Although dichloromethane is not controlled under the Montreal Protocol, it has been identified as a source of atmospheric chlorine [1]. Despite its prevalence as a laboratory solvent, it is linked to serious acute and long-term health issues [2].

In 1952, the first microwave study of CH_2Cl_2 reported the spectra of seven isotopologues ($CH_2^{35}Cl_2$, $CH_2^{35}Cl^{37}Cl$, $CH_2^{37}Cl_2$, $CDH^{35}Cl_2$, $CDH^{35}Cl^{37}Cl$, $CD_2^{35}Cl_2$, $CD_2^{35}Cl^{37}Cl$) [3]. The molecular structure, dipole moment ($\mu_b = 1.62$ D), and nuclear quadrupole coupling constants of dichloromethane were determined. Subsequently, Harmony and collaborators observed the spectrum of $^{13}CH_2Cl_2$ for the first time and the spectra of other isotopologues with higher precision, providing the first substitution structure (r_s) [4]. Later, the microwave spectrum of CH_2Cl_2 was measured from 14 to 75 GHz with rotational transitions up to $J' = 80$ [5], allowing a partial determination of the sextic centrifugal distortion constants using an A-reduced Hamiltonian in the I^r representation. Pure rotational transitions were observed in the far-infrared spectrum of CH_2Cl_2 between 10 and 75 cm^{-1} for the ground vibrational states of $CH_2^{35}Cl_2$ and $CH_2^{35}Cl^{37}Cl$ and ν_4 of $CH_2^{35}Cl_2$, providing A-reduced spectroscopic constants up to the octic level [6]. Kisiel *et al.* re-investigated the nuclear quadrupole hyperfine structure in the microwave transitions, providing precise and accurate nuclear quadrupole coupling constants and nuclear spin-rotation constants for the chlorine nuclei [7]. Very recently, the rotational spectra were extended up to 1.1 THz [8], providing well-determined spectroscopic and centrifugal distortion constants through the octic level. Dichloromethane has two identical chlorine nuclei (nuclear spin $\frac{3}{2}$), which create readily observable splitting of the rotational transitions, as well as two identical hydrogen nuclei (nuclear spin $\frac{1}{2}$) whose smaller splittings have never been resolved. The rotational levels are split up to 16 levels by the nuclear spin of chlorine, but most of the rotational transitions split into three measurable components with a strong central line. In the THz study [8], however, the frequencies of the center were analyzed without considering hyperfine structure. Very recently, rotational spectra of the ground state, $\nu_4 = 1$, 2, 3, $\nu_3 = 1$, and $\nu_9 = 1$ vibrationally excited states have been reported by FT-MW [9].

The low-resolution infrared spectra below 6200 cm^{-1} were studied,

☆ This article is part of a special issue entitled: 'Student Research' published in Journal of Molecular Spectroscopy.

* Corresponding author.
E-mail address: kaori@sci.u-toyama.ac.jp (K. Kobayashi).

https://doi.org/10.1016/j.jms.2024.111982
Received 20 August 2024; Received in revised form 24 October 2024; Accepted 17 December 2024
Available online 20 December 2024
0022-2852/© 2024 Elsevier Inc. All rights are reserved, including those for text and data mining, AI training, and similar technologies.

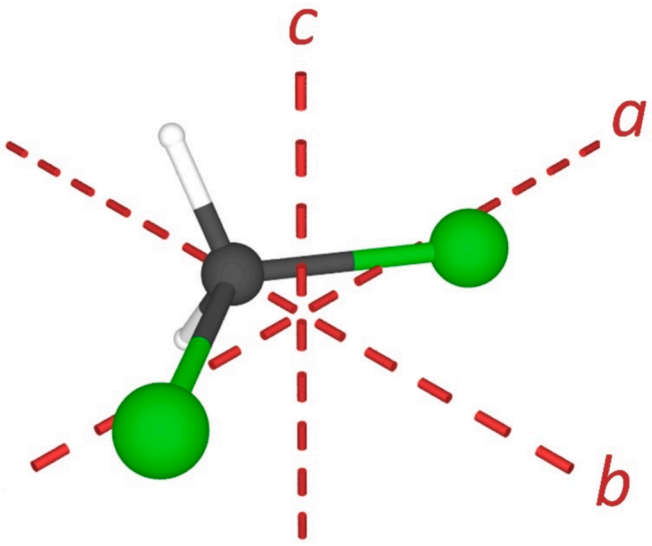

Fig. 1. Dichloromethane structure (C_{2v}, μ_b = 1.62 D [3]) with principal inertial axes.

and an empirical harmonic force field was obtained by Duncan *et al.* [10,11]. Tullini *et al.* studied high-resolution vibration–rotation spectra of ν_2, ν_7, ν_8, and $\nu_2 + \nu_8$ [12]. Snels and coworkers also extensively studied the ν_8, $2\nu_8$, $\nu_2 + \nu_8$, ν_3, ν_9, $\nu_4 + \nu_8$, and $2\nu_4 + \nu_8 - \nu_4$ (hot band) [13–16]. The Raman spectroscopic study by Escribano *et al.* observed the lowest vibrational excited state (ν_4, CCl_2 scissoring mode) at 281.5 cm^{-1} [17].

In this paper, we report the rotational spectroscopy of $CH_2^{35}Cl_2$ in the ground and ν_4 vibrational states. The relative intensity of ν_4 transitions is predicted to be 26% compared to the ground state, assuming the Boltzmann distribution at 300 K. The frequencies of transitions showing hyperfine splitting are accurately measured and analyzed. Many additional transitions are visible in the spectrum from other vibrationally excited states of $CH_2^{35}Cl_2$ and the ground and vibrationally excited states of $CH_2^{35/37}Cl_2$ and $CH_2^{37}Cl_2$. The spectra of these species will be addressed in a subsequent work.

2. Methods

2.1. Experimental

Our rotational spectra were collected with three different spectrometers, using a commercial sample of dichloromethane (Spectrochemical Analysis grade 99.9+% FUJIFILM Wako Chemicals in Toyama and Sigma-Adrich in Wisconsin). The microwave spectra near 11.3 GHz were observed by using the chirped-pulse Fourier-transform microwave spectrometer (CP-FTMW) at the University of Toyama. The broadband spectra from 29 to 75 GHz were observed by using the conventional source-modulation microwave spectrometer at the University of Toyama. Broadband spectra from 85 to 750 GHz were collected at the University of Wisconsin-Madison.

The CP-FTMW spectrometer was built based on the design of McJunkins and Brown [18], which is a less expensive spectrometer of similar design to the one described by Shipman *et al.* [19]. The waveguide appropriate for the frequency region was used to measure the room temperature spectra with sample pressures between 15–50 mTorr. The chirp span was 100 MHz with 50,000 molecular signal acquisitions. The sample pressure was about 5 mTorr and the linewidth was about 400 kHz with a nominal measurement uncertainty of 20 kHz. The 40 to 75 GHz spectral region was collected with a previously described spectrometer from the University of Toyama [20,21] that has been upgraded with a GPS frequency lock. The 26 to 40 GHz radiation was output from an Agilent E8257D signal generator with a frequency doubler (Spacek Labs Ka-2). Instead of the InSb detector, we used multiple broadband waveguide detectors (Hewlett-Packard R422C, Spacek Labs DQ-2, Virginia Diodes WR15ZBD) in the 26 to 75 GHz region. Most of the spectra were obtained at room temperature but a limited number of measurements were observed at dry ice temperature to improve intensity of low J, K transitions. The spectra from 85 to 750 GHz were collected using a millimeter-wave spectrometer at the University of Wisconsin – Madison that has been previously described [22], in a continuous flow at room temperature, with sample pressures of 3 to 8 mTorr. The complete spectrum from 85 to 750 GHz was obtained automatically over approximately fourteen days using the following experimental parameters: 0.6 MHz/*sec* sweep rate, 10 ms time constant, and 50 kHz AM and 500 kHz FM modulation in a tone-burst design. A uniform frequency measurement uncertainty of 0.050 MHz was assumed for all measurements from 26 to 750 GHz.

2.2. Spectroscopic analysis

The separate segments of the rotational spectrum were combined into a single broadband spectrum using Kisiel's Assignment and Analysis of Broadband Spectra (AABS) software [23,24], except CP-FTMW data. Pickett's SPFIT/SPCAT [25] were used for least-squares fitting and spectral predictions, along with Kisiel's PIFORM, PLANM, and AC programs for analysis [26]. The center frequencies of the data obtained by CP-FTMW were determined separately and added to the above analysis.

2.3. Computational

Electronic structure calculations were carried out with Gaussian 16 [27] to obtain theoretical spectroscopic constants. The optimized geometry at the B3LYP/6–311+G(2d,p) level was obtained using "very-tight" convergence criteria and an "ultrafine" integration grid, and subsequent anharmonic vibrational frequency calculations were carried out. Computational output files can be found in the Supplementary Material.

3. Analysis and results

3.1. Vibrational ground state

Dichloromethane is a highly prolate, asymmetric top (C_{2v}, $\kappa = -0.982$, Fig. 1) with a b-axis dipole, $\mu_b = 1.62$ D [3]. The presence of two chlorine nuclei ($I = \frac{3}{2}$) causes splitting of the rotational transitions due to nuclear quadrupole and nuclear spin-rotation interactions. Similar to a previous study [5], the measured rotational transitions were least-squares fit to a partial octic, A-reduced Hamiltonian in the I^r representation. Due to the highly prolate nature of dichloromethane, and the known propensity for the A-reduced Hamiltonian to breakdown for highly prolate molecules in the I^r representation [28–30], we also provide a least-squares fit the rotational transitions to a partial octic, S-reduced Hamiltonian in the I^r representation. As in preceding studies [6,7], our final data sets for both the ground state and ν_4 included many hyperfine-resolved and many hyperfine-unresolved transitions. Hyperfine-resolved transitions were assigned quantum numbers using the following coupling scheme.

$$I_{Cl1} + I_{Cl2} = I_{total}$$
$$J + I_{total} = F$$

The nuclear spin-rotation of chlorine nuclei (M_{cc}) was included in the Hamiltonian, similar to previous work [7].

Fig. 2 shows an example microwave transition ($J' = 10_{0,10} \leftarrow J'' = 9_{1,9}$) with resolvable nuclear-hyperfine coupling at 40.069 GHz recorded at the University of Toyama. The simulation in the figure was reproduced from our spectroscopic constants, assuming a second-

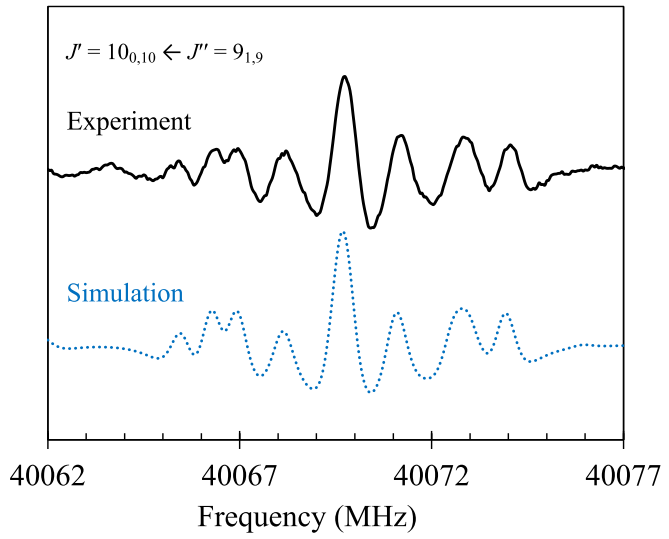

Fig. 2. The hyperfine-resolved transition ($J' = 10_{0,10} \leftarrow J'' = 9_{1,9}$) in the ground state of $CH_2^{35}Cl_2$ observed at room temperature. The solid line and dotted line represent the experimental spectrum and simulation, respectively. The simulation was reproduced from the experimental spectroscopic constants, assuming second derivative form of a Lorentzian profile with the linewidth of 0.7 MHz.

derivative Lorentzian line shape with a linewidth of 0.7 MHz. Table 1 provides the quantum number assignments, transition frequencies and *obs.–calc.* values for these transitions. With repeated assignments using AABS and analysis and prediction with SPFIT/SPCAT, the assignments were mostly straightforward. While proceeding with the fitting, however, it was sometimes necessary to revise the assignment of hyperfine-resolved transitions. This is probably due to local heavy mixing of wavefunctions resulting in the unstable selection of quantum numbers in the program and small changes in the nuclear quadrupole coupling constants between least-squares fitting iterations.

A total of 3170 hyperfine-resolved and 2296 hyperfine-unresolved transitions, including the FT-MW data by Kisiel *et al.* [7], were in included in our final ground state data set, Fig. 3. As inferred from the data distribution plot, all transitions with *obs.–calc.* values greater than three times the nominal measurement uncertainty of 50 kHz were excluded from the data set. There is no discernible systematic pattern in the location of the larger symbols, which correspond to the relatively high *obs.–calc.* transitions remaining in the data set. The hyperfine-resolved transitions include J'' quanta from 1 to 105 and K_a'' from 0 to 16. The hyperfine-unresolved transitions span a larger range of J'' and K_a'' quanta, from 10 to 119 for J'' and from 0 to 21 for K_a''.

The computed and experimental spectroscopic constants of ground state dichloromethane are summarized in Table 2. The data set was least-squares fit to partial octic, centrifugally distorted A- and S-reduced Hamiltonians using the I^r representation. These values were determined from combined least-squares fits of the rotational transitions from the ground and ν_4 vibrational state. The combined least-squares fit allowed overlapping transitions from each state to be included. In the A-reduction, the l_k constant could not be determined from the current data set and was held constant at its previously reported value Ulenikov *et al.* [8]. Floating l_k increases the error of L_{JK}, suggesting strong correlation between these parameters. In contrast to the fit presented in reference [6], a complete set of diagonal octic constants was determined in this study. We present the S-reduction spectroscopic constants of dichloromethane for the first time in this work. The parallel analysis of the S-reduction least-squares fit indicates that the A-reduction least-squares fit is treating the data set well, despite the aforementioned highly prolate structure of dichloromethane. In either reduction, there are not any systematic quantum number trends in the transitions with high *obs.–calc.* values, and both least-squares fits have a σ_{fit} value of 0.046 MHz, indicating that both reductions model the data set equally well. In either reduction, the computed quartic centrifugal distortion constants have discrepancies with the experimental values of 3 to 12%, with the largest discrepancy occurring for d_2, which has a much smaller absolute value than the other constants. The computed sextic centrifugal distortion constants have similar discrepancies ranging from 2 to 15%, with two notable exceptions. The computed values of Φ_{JK} and H_{JK} differ by 27% and 117%, respectively. These computed constants are likely impacted by an error in their estimation described in a previous work [31].

3.2. *Vibrationally excited state ν_4*

The spectroscopic constants obtained for ν_4 are summarized in Table 3, which includes a determination of its nuclear-coupling constants for the first time. The data set of ν_4 contains 2025 hyperfine-resolved transitions, where J is from 1 to 92, and K from 0 to 15, and 1584 hyperfine-unresolved transitions of J from 7 to 114, and K_a from 0 to 20. Similar to the ground state, these data were fit to partial octic, centrifugally distorted A- and S-reduced Hamiltonians in the I^r representation. The rotational and centrifugal distortion constants (up to the sextic level) of ν_4 display the expected small deviations from their corresponding ground state values. The quartic centrifugal distortion constants change by 0.2% to9 % in both reductions, with the greatest deviations occurring for δ_K and d_2. The sextic centrifugal distortion constants show slightly larger changes compared to their corresponding ground state values of 3 to 18%. The A-reduction octic constant L_{JK} changes by 186% compared to its ground-state value. This suggests that the value of L_{JK} of ν_4 is simply a fitting constant in the least-squares fit (i.e. an 'effective' constant) rather than a physically meaningful centrifugal distortion constant. The inability to determine the constants L_J and

Table 1
Nuclear-hyperfine-resolved components of the ground state rotational transition, $J' = 10_{0,10} \leftarrow J'' = 9_{1,9}$ of dichloromethane ($CH_2^{35}Cl_2$).

J'	*Ka'*	*Kc'*	*I'*	*F'*	*J"*	*Ka"*	*Kc"*	*I"*	*F"*	Frequency (MHz)	*obs. –calc.* (MHz)	*obs. –averaged calc.*(MHz)
10	0	10	3	7	9	1	9	3	6	40065.410	−0.069	
10	0	10	1	10	9	1	9	1	9	40066.389	0.115	0.115
10	0	10	2	10	9	1	9	0	9		0.114	
10	0	10	3	13	9	1	9	3	12	40066.952	0.022	
10	0	10	3	8	9	1	9	3	7	40068.208	0.070	
10	0	10	3	9	9	1	9	3	8	40069.733	0.200	0.046
10	0	10	1	11	9	1	9	1	10		0.070	
10	0	10	2	11	9	1	9	2	10		−0.065	
10	0	10	2	12	9	1	9	2	11		−0.059	
10	0	10	2	9	9	1	9	2	8		−0.080	
10	0	10	2	8	9	1	9	2	7		−0.082	
10	0	10	3	12	9	1	9	3	11	40071.200	0.111	
10	0	10	1	9	9	1	9	1	8	40072.841	0.271	0.067
10	0	10	1	9	9	1	9	1	8		−0.121	
10	0	10	3	11	9	1	9	3	10	40074.051	0.136	

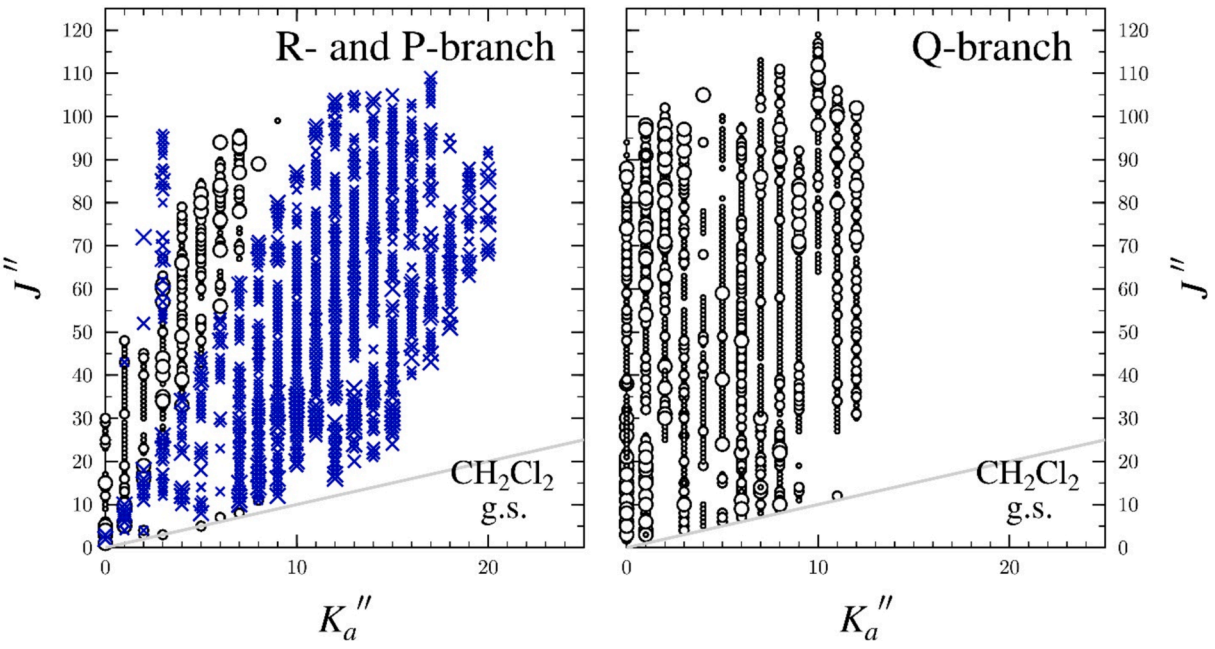

Fig. 3. Data distribution plot for the least-squares fit of spectroscopic data for the vibrational ground state of dichloromethane ($CH_2^{35}Cl_2$). Black circles are used for R- and Q-branch transitions. Blue crosses are used for P-branch transitions. The size of the symbol is proportional to the value of $|(f_{obs.} - f_{calc.})/\delta f|$, where δf is the frequency measurement uncertainty, and all quotient values are smaller than 3.

Table 2
Spectroscopic constants of dichloromethane ($CH_2^{35}Cl_2$) in its ground vibrational state using A- and S-reduced Hamiltonians, I^r representation.

A-reduced	B3LYP	Current Study	Ulenikov *et al.* [8]	Kisiel *et al.* [7]	S-reduced	B3LYP	Current Study
A_0/MHz	31,785	32002.29301 (25)	32002.28977 (11)	[32002.2900][a]	A_0/MHz	31,785	32002.29310 (25)
B_0/MHz	3198	3320.281838 (41)	3320.281213 (16)	3320.28126 (6)	B_0/MHz	3198	3320.271022 (41)
C_0/MHz	2959	3065.229690 (42)	3065.229086 (16)	[3065.22985][a]	C_0/MHz	2959	3065.240469 (42)
Δ_J/kHz	1.330	1.394961 (13)	1.3948703 (37)	[1.396724][a]	D_J/kHz	1.319	1.383031 (13)
Δ_{JK}/kHz	−25.10	−26.11408 (15)	−26.113701 (86)	[−26.0789][a]	D_{JK}/kHz	−25.03	−26.04278 (15)
Δ_K/kHz	491.8	472.9214 (18)	472.92776 (74)	[472.959][a]	D_K/kHz	491.8	472.8633 (18)
δ_J/kHz	0.1621	0.17703496 (82)	0.17703853 (88)	[0.177219][a]	d_1/kHz	−0.1621	−0.17703318 (84)
δ_K/kHz	5.169	5.40321 (20)	5.40343 (28)	[5.2985][a]	d_2/kHz	−0.005272	−0.00596361 (22)
Φ_J/Hz	0.0008619	0.0008952 (16)	0.00088445 (31)		H_J/Hz	0.0008166	0.0008439 (16)
Φ_{JK}/Hz	0.008774	0.012088 (36)	0.011708 (62)		H_{JK}/Hz	−0.0002537[b]	0.001486 (28)
Φ_{KJ}/Hz	−1.782	−1.74131 (39)	−1.73888 (33)		H_{KJ}/Hz	−1.751	−1.70628 (38)
Φ_K/Hz	24.79	23.0578 (70)	23.0810 (26)		H_K/Hz	24.77	23.0393 (70)
ϕ_J/Hz	0.0002656	0.000284111 (72)	0.00028436 (14)		h_1/Hz	0.0002632	0.000281498 (71)
ϕ_{JK}/Hz	0.003505	0.003702 (28)	0.003940 (78)		h_2/Hz	0.00002261	0.000025123 (30)
ϕ_K/Hz	1.469	1.5711 (34)	1.5069 (89)		h_3/Hz	0.000002371	0.0000028214 (60)
L_J/mHz		−0.000000481 (62)			L_J/mHz		−0.000000401 (62)
L_{JJK}/mHz		−0.0000593 (14)	−0.0000615 (14)		L_{JJK}/mHz		−0.0000174 (14)
L_{JK}/mHz		0.002989 (33)	0.0307 (71)		L_{JK}/mHz		−0.002404 (34)
L_{KKJ}/mHz		0.11214 (69)	0.1086 (22)		L_{KKJ}/mHz		0.12609 (69)
L_K/mHz		−1.546 (10)	−1.5528 (37)		L_K/mHz		−1.555 (10)
l_K/mHz		[0.582][c]	0.582 (69)				
$\frac{3}{2}\chi_{aa}$/MHz	−60.7	−62.6105 (21)		−62.6127 (17)	$\frac{3}{2}\chi_{aa}$/MHz	−60.7	−62.6105 (21)
$\frac{1}{4}(\chi_{bb}-\chi_{cc})$/MHz	−9.4	−9.53329 (75)		−9.53528 (55)	$\frac{1}{4}(\chi_{bb}-\chi_{cc})$/MHz	−9.4	−9.53330 (75)
χ_{ab}/MHz	51.7	51.50 (29)		50.93 (23)	χ_{ab}/MHz	51.7	51.50 (29)
M_{cc}/MHz		[0.00188][d]		0.00188 (15)	M_{cc}/MHz		[0.00188][d]
σ_{fit}/MHz		0.046[e]	0.019	0.00128	σ_{fit}/MHz		0.046[e]
J_{max}		119	107	3	J_{max}		119
K_{max}		21	20	1	K_{max}		21
N_{lines}		5447	4502	47	N_{lines}		5447

[a] Held at the value from reference [6].
[b] Value miscalculated as described in reference [29].
[c] Held constant at the value from reference [8].
[d] Held constant at the value from reference [7].
[e] This rms was obtained by the combined fit of the ground state and ν_4.

Table 3
Spectroscopic constants of dichloromethane ($CH_2^{35}Cl_2$) in its ν_4 vibrational state using A- and S-reduced Hamiltonians, I^r representation.

A-reduced	Current Study	Tullini *et al.* [6]	S-reduced	Current Study
A_v/MHz	32197.34012 (36)	32197.2192 (207)	A_v/MHz	32197.33990 (34)
B_v/MHz	3317.700106 (40)	3317.68271 (249)	B_v/MHz	3317.688270 (40)
C_v/MHz	3060.928776 (39)	3060.91481 (246)	C_v/MHz	3060.940580 (39)
Δ_J/kHz	1.3875268 (84)	1.35785 (93)	D_J/kHz	1.3744784 (85)
Δ_{JK}/kHz	−26.17136 (26)	−26.1278 (147)	D_{JK}/kHz	−26.09364 (17)
Δ_K/kHz	488.3307 (31)	487.9932 (340)	D_K/kHz	488.2661 (31)
δ_J/kHz	0.1767497 (12)	0.17678 (14)	d_1/kHz	−0.1767479 (12)
δ_K/kHz	5.91363 (32)	5.6601 (809)	d_2/kHz	−0.00652604 (36)
Φ_J/Hz	0.00086476 (49)	0.0010193 (899)	H_J/Hz	0.00081204 (51)
Φ_{JK}/Hz	0.014598 (86)	−0.02182 (279)	H_{JK}/Hz	0.001713 (23)
Φ_{KJ}/Hz	−1.80551 (93)	−1.5784 (102)	H_{KJ}/Hz	−1.76175 (89)
Φ_K/Hz	24.724 (14)	24.048 (25)	H_K/Hz	24.693 (14)
ϕ_J/Hz	0.00028045 (12)	[0.0002938]	h_1/Hz	0.00027716 (12)
ϕ_{JK}/Hz	0.003051 (55)	[0.0]	h_2/Hz	0.000026508 (60)
ϕ_K/Hz	1.8902 (88)	[−4.29][a]	h_3/Hz	0.000003425 (15)
L_J/mHz		[−0.0000063136][a]	L_J/mHz	
L_{JJK}/mHz	−0.0000605 (45)	[0.0]	L_{JJK}/mHz	
L_{JK}/mHz	−0.003493 (98)	[0.0]	L_{JK}/mHz	−0.002726(98)
L_{KKJ}/mHz	0.1438 (22)	[0.0582][a]	L_{KKJ}/mHz	0.1398(22)
L_K/mHz	−1.817 (27)	[−1.3421][a]	L_K/mHz	−1.814(27)
$\frac{3}{2}\chi_{aa}$/MHz	−63.033 (71)		$\frac{3}{2}\chi_{aa}$/MHz	−63.035 (71)
$\frac{1}{4}(\chi_{bb}-\chi_{cc})$/MHz	−9.4804 (40)		$\frac{1}{4}(\chi_{bb}-\chi_{cc})$/MHz	−9.4808 (40)
χ_{ab}/MHz	[50.93][b]		χ_{ab}/MHz	[50.93][b]
M_{cc}/MHz	[0.00188][b]		M_{cc}/MHz	[0.00188][b]
σ_{fit}/MHz	0.046[c]	0.72	σ_{fit}/MHz	0.046[c]
J_{max}	114	67	J_{max}	114
K_{max}	20	31	K_{max}	20
N_{lines}	3609	1260	N_{lines}	3609

[a] Held at the ground state value from reference [6].
[b] Held constant at the value from reference [7].
[c] This rms was obtained by the combined fit of the ground state and ν_4.

L_K likely precludes the ability to determine L_{JK}. All other octic centrifugal distortion terms are likely to have some physical meaning since the deviations between ν_4 and the ground state are modest (10 to 22%). The previously reported value of Φ_{JK} is clearly an effective constant as it differs by 250% from the value determined in this work and from the corresponding ground-state value by 280%. The nuclear-coupling cross term χ_{ab} could not be determined for ν_4, thus its value was held at its ground-state value. As expected, the remaining ν_4 nuclear-coupling constants were in close agreement with their ground state counterparts, differing by less than 1%.

4. Discussion

The determination of rotational constants for both the ground state and ν_4 provides the vibration–rotation interaction constants of ν_4 summarized in Table 4. The B3LYP computed values are in good agreement and vary by at most 1.6%. This is consistent with other studies of vibrationally excited states that do not display Coriolis-coupling with near-energy vibrational states [32–34].

We performed fittings with nuclear-hyperfine constants held at the values obtained in the study of the ground state by Kisiel [7] *et al.* (Supplementary Material) or with those constants allowed to vary (Table 2). When the hyperfine constants were allowed to vary for both states, it was not possible to obtain a converged least-squares fit with M_{cc} in either state or χ_{ab} for ν_4. Therefore, those constants are held at the values obtained by the FT-MW study [7]. About 0.4% of the measured lines were excluded from the fit, and most transitions are thought to be excluded by the overlap with the $^{35}Cl^{37}Cl$ and $^{37}Cl^{37}Cl$ isotopologues and their vibrationally excited states. Floating additional centrifugal distortion or nuclear-hyperfine constants did not improve the number of lines included in the fit and only slightly improved σ_{fit}. As shown in Tables 2 and 3, our spectroscopic constants are generally in good agreement with the previous studies [3,5–7], considering the accuracy and frequency regions. The spectroscopic constants of Ulenikov *et al.* [8], however, disagree with those found in this study within the 2σ statistical uncertainties of each set of values. This is likely due to the greater frequency range covered in that work (up to 1.1 THz) and the inclusion of the nuclear-hyperfine constants in this work. Given the precision of the hyperfine-resolved FT-MW data and their inclusion in the data set of this work, it is expected that the values determined by Kisiel *et al.* [7] and our work would be in close agreement. Indeed, $\frac{3}{2}\chi_{aa}$ and χ_{ab} agree within the 1σ statistical uncertainties of each value while $\frac{1}{4}(\chi_{bb}-\chi_{cc})$ agrees within 2σ statistical uncertainties and differs by only 0.021%. The B3LYP computed values of $\frac{3}{2}\chi_{aa}$, $\frac{1}{4}(\chi_{bb}-\chi_{cc})$, and χ_{ab} are all within 3% of their experimental values (Table 2).

Dichloromethane (CH_2Cl_2) is a potential candidate for detection as an interstellar molecule, because the closely related species chloromethane (CH_3Cl) was detected in the low-mass protostellar source in IRAS 16293B as a result of the increased sensitivity of ALMA [35] relative to previous telescopes. Additionally, both CH_3Cl and CH_2Cl_2 were detected from Martian soil samples [36], supporting the potential for detection of CH_2Cl_2 in interstellar space. For astronomical applications, it is essential to have appropriate line parameters and partition functions. The list of the transitions will be deposited in the Toyama Microwave Atlas. The partition function for the ground state of dichloromethane (CH_2Cl_2) at 300 K is provided in the Jet-Propulsion Lab (JPL) catalog [37], and is 13,929,632, which is 9 times larger than the

Table 4
Vibration-Rotation Interaction Constants of ν_4 of dichloromethane ($CH_2^{35}Cl_2$).

	Experimental [a]	B3LYP [b]	*obs.* –B3LYP.
$A_0 - A_4$ (MHz)	−195.04711 (44)	−193.4	−1.6
$B_0 - B_4$ (MHz)	2.581732 (57)	2.28	0.30
$C_0 - C_4$ (MHz)	4.300914 (57)	4.00	0.30

[a] Determined from the A-reduction rotational constants.
[b] Evaluated with the 6–311+G(2d,p) basis set.

value numerically calculated from our spectroscopic constants, 1,557,822. The calculation is explained in the appendix. The difference from the JPL value is unclear, and the resultant smaller partition function indicates the higher possibility of astronomical observations.

5. Conclusion

We provide transition frequencies for dichloromethane (CH_2Cl_2) across the frequency range of modern radio telescopes. This work is a significant extension of the hyperfine-resolved transitions to the higher frequency range up to 750 GHz. Additionally, the spectroscopic constants provided in this work, including the nuclear quadrupole coupling constants, provide the ability to predict transition frequencies accurately at lower frequencies and slightly higher frequencies. The comparison of the computed spectroscopic constants to the experimental values reveals an error in the determination of the computed values of Φ_{JK} and H_{JK}.

CRediT authorship contribution statement

Manamu Kobayashi: Writing – original draft, Visualization, Investigation, Formal analysis. **Kaori Kobayashi:** Writing – review & editing, Writing – original draft, Supervision, Investigation, Formal analysis, Conceptualization. **Brian J. Esselman:** Writing – review & editing, Writing – original draft, Investigation, Formal analysis. **R.Claude Woods:** Writing – review & editing, Investigation. **Robert J. McMahon:** Writing – review & editing, Investigation. **Satoshi Yamamoto:** Writing – review & editing, Formal analysis. **Hiroyuki Ozeki:** Writing – review & editing, Formal analysis.

Declaration of competing interest

The authors declare that they have no known competing financial interests or personal relationships that could have appeared to influence the work reported in this paper.

Acknowledgments

KK thanks the support from the Grant-in-Aid for Scientific Research on Innovative Areas by the Ministry of Education, Culture, Sports, Science, and Technology of Japan (Grant No. 21H00038), and National Astronomical Observatory of Japan. The Wisconsin group gratefully acknowledges the National Science Foundation for its support of this project (CHE-2245738).

Appendix: Partition function

In the Supplementary table, we list the partition function (Q) from the approximate relation calculated by using the following equation [38], and that from numerical calculation using our hyperfine-resolved molecular constants, considering up to F =129.

$$Q = Q_{nuc.}Q_{rot.}Q_{vib.} \cong \frac{64}{\sigma}\left(\frac{\pi(kT)^3}{ABC}\right)^{1/2}\prod_i \frac{1}{1-e^{-hc\omega_i/kT}}$$

In the nuclear spin partition function (Q_{nuc}), there are 64 nuclear spin states, only half of which are allowed for this C_{2v} molecule as explained in the previous paragraph leading to a symmetry number (σ) of 2. In the rotational and vibrational partition functions (Q_{rot} and Q_{vib}), k, T, and ω_i are the Boltzmann constant, temperature, and the i^{th} harmonic vibrational frequency which runs over all the normal modes. In the case of dichloromethane, the only vibrational frequency below 500 cm^{-1} is important, as a result the populations of other vibrational modes are negligible. The results with and without including the ν_4 vibration differ above 37.5 K, when the ν_4 vibrational state begins to be populated. In the interstellar medium, the inclusion of the vibrational partition function may or may not be relevant given the low temperatures and lack of thermal equilibrium, *i.e.*, the rotational and vibrational temperature are not the same. Thus, the ground state only partition functions are also included.

Appendix A. Supplementary data

Supplementary data for this article are available on Science Direct (www.sciencedirect.com) and as part of the Ohio State University Molecular Spectroscopy Archives (http://msa.lib.ohio-state.edu/jmsa_hp.htm). Supplementary data to this article can be found online at https://doi.org/10.1016/j.jms.2024.111982.

Data availability

Data will be made available on request.

References

[1] World Meteorological Organization Global Ozone Research and Monitoring Project - Report No. 58, Scientific Assessment of Ozone Depletion: 2018.
[2] K. Vasquez, A reckoning for methylene chloride in academic labs, C&EN Glob. Enterp. 102 (2024) 22–27, https://doi.org/10.1021/cen-10221-cover1.
[3] R.J. Myers, W.D. Gwinn, The Microwave Spectra, Structure, Dipole Moment, and Chlorine Nuclear Quadrupole Coupling Constants of Methylene Chloride, J. Chem. Phys. 20 (1952) 1420–1427, https://doi.org/10.1063/1.1700773.
[4] M.D. Harmony, S.N. Mathur, S.J. Merdian, Microwave spectrum and substitution structure of methylene chloride, J. Mol. Spectrosc. 75 (1979) 144–149, https://doi.org/10.1016/0022-2852(79)90155-3.
[5] R.W. Davis, A.G. Robiette, M.C.L. Gerry, The harmonic force fields of methylene chloride and dichlorosilane from combined microwave and infrared data, J. Mol. Spectrosc. 85 (1981) 399–415, https://doi.org/10.1016/0022-2852(81)90212-5.
[6] F. Tullini, G.D. Nivellini, M. Carlotti, B. Carli, The far-infrared spectrum of methylene chloride, J. Mol. Spectrosc. 138 (1989) 355–374, https://doi.org/10.1016/0022-2852(89)90004-0.
[7] Z. Kisiel, J. Kosarzewski, L. Pszczółkowski, Nuclear Quadrupole Coupling Tensor of CH_2Cl_2 : Comparison of Quadrupolar and Structural Angles in Methylene Halides, Acta Phys. Pol. a. 92 (1997) 507–516, https://doi.org/10.12693/APhysPolA.92.507.
[8] O.N. Ulenikov, O.V. Gromova, E.S. Bekhtereva, H.S.P. Müller, L. Margulès, Submillimeter wave spectrum of methylene chloride, $^{12}CH_2^{35}Cl_2$, $^{12}CH_2^{35}Cl^{37}Cl$ and $^{12}CH_2^{37}Cl_2$ up to 1.1 THz, J. Quant. Spectrosc. Radiat. Transf. 319 (2024) 108962, https://doi.org/10.1016/j.jqsrt.2024.108962.
[9] Z. Kisiel, Isotopic species, vibrational states and nuclear quadrupole splitting in CH_2Cl_2 from rotational spectroscopy at 8–18 GHz, J. Mol. Spectrosc. (2024) 111954, https://doi.org/10.1016/j.jms.2024.111954.
[10] J.L. Duncan, G.D. Nivellini, F. Tullini, Methylene chloride: The mid-infrared spectrum of an almost vibrationally unperturbed molecule, J. Mol. Spectrosc. 118 (1986) 145–162, https://doi.org/10.1016/0022-2852(86)90231-6.
[11] J.L. Duncan, D.A. Lawie, G.D. Nivellini, F. Tullini, A.M. Ferguson, J. Harper, K. H. Tonge, The empirical general harmonic force field of methylene chloride, J. Mol. Spectrosc. 121 (1987) 294–303, https://doi.org/10.1016/0022-2852(87)90053-1.
[12] F. Tullini, M. Dinelli, G.D. Nivellini, J.L. Duncan, High resolution vibration—rotation analyses for methylene chloride, Spectrochim. Acta Part A Mol, Spectrosc. 42 (1986) 1165–1169, https://doi.org/10.1016/0584-8539(86)80070-8.

[13] A. Morone, M. Snels, O. Polanz, High-Resolution Spectra and Analysis of the ν_8 Band of Methylene Chloride, J. Mol. Spectrosc. 173 (1995) 113–119, https://doi.org/10.1006/jmsp.1995.1223.
[14] M. Snels, High Resolution Spectra and Rotational Analysis of the $2\nu_8$, $\nu_2+\nu_8$, and $2\nu_2$ Bands in Methylene Chloride, J. Mol. Spectrosc. 182 (1997) 124–131, https://doi.org/10.1006/jmsp.1996.7198.
[15] M. Snels, High Resolution IR Study of the Coriolis Coupling between ν_3 and ν_9 in $CH_2^{35}Cl^{37}Cl$, J. Mol. Spectrosc. 183 (1997) 224–227, https://doi.org/10.1006/jmsp.1997.7263.
[16] M. Snels, G. D'amico, High resolution FTIR spectra and analysis of the $\nu_4+\nu_8$ combination band and of the $2\nu_4+\nu_8-\nu_4$ hot band of $CH_2^{35}Cl_2$, Mol. Phys. 101 (2003) 799–803, https://doi.org/10.1080/0026897021000044043.
[17] R. Escribano, J.M. Orza, S. Montero, C. Domingo, Absolute Raman intensities, force constants, and electro-optical parameters of CH_2Cl_2, CD_2Cl_2 and $CHDCl_2$, Mol. Phys. 37 (1979) 361–377, https://doi.org/10.1080/00268977900100321.
[18] A. McJunkins, G.G. Brown, An inexpensive room-temperature chirped pulse fourier transform microwave (RT-CP-FTMW) spectrometer, J. Undergrad. Chem. Res. 10 (2011) 158–161.
[19] B. Reinhold, I.A. Finneran, S.T. Shipman, Room temperature chirped-pulse Fourier transform microwave spectroscopy of anisole, J. Mol. Spectrosc. 270 (2011) 89–97, https://doi.org/10.1016/j.jms.2011.10.002. 2.
[20] Y. Fukuyama, H. Odashima, K. Takagi, S. Tsunekawa, Y. Fukuyama, H. Odashima, K. Takagi, S. Tsunekawa, The Microwave Spectrum of Propionitrile (C_2H_5CN) in the Frequency Range from 8 to 200 GHz, Astrophys. J. Suppl. Ser. 104 (1996) 329, https://doi.org/10.1086/192303.
[21] K. Kobayashi, K. Takamura, Y. Sakai, S. Tsunekawa, H. Odashima, N. Ohashi, The microwave spectroscopy of methyl formate in the second torsional excited state, Astrophys. J., Suppl. Ser. 205 (2013) 9, https://doi.org/10.1088/0067-0049/205/1/9.
[22] B.J. Esselman, M.A. Zdanovskaia, H.H. Smith, R.C. Woods, R.J. McMahon, The 130–500 GHz Rotational Spectroscopy of Cyanopyrazine ($C_4H_3N_2$-CN), J. Mol. Spectrosc. 389 (2022) 111703, https://doi.org/10.1016/j.jms.2022.111703.
[23] Z. Kisiel, L. Pszczółkowski, I.R. Medvedev, M. Winnewisser, F.C. De Lucia, E. Herbst, Rotational spectrum of *trans-trans* diethyl ether in the ground and three excited vibrational states, J. Mol. Spectrosc. 233 (2005) 231–243, https://doi.org/10.1016/j.jms.2005.07.006.
[24] Z. Kisiel, L. Pszczółkowski, B.J. Drouin, C.S. Brauer, S. Yu, J.C. Pearson, I. R. Medvedev, S. Fortman, C. Neese, Broadband rotational spectroscopy of acrylonitrile: Vibrational energies from perturbations, J. Mol. Spectrosc. 280 (2012) 134–144, https://doi.org/10.1016/J.JMS.2012.06.013.
[25] H.M. Pickett, The fitting and prediction of vibration-rotation spectra with spin interactions, J. Mol. Spectrosc. 148 (1991) 371–377, https://doi.org/10.1016/0022-2852(91)90393-O.
[26] Kisiel, Z. PROSPE - Programs for ROtational SPEctroscopy. http://info.ifpan.edu.pl/~kisiel/prospe.htm (accessed August 2024).
[27] Frisch, M. J.; Trucks, G. W.; Schlegel, H. B.; Scuseria, G. E.; Robb, M. A.; Cheeseman, J. R.; Scalmani, G.; Barone, V.; Petersson, G. A.; Nakatsuji, H.; Li, X.; Caricato, M.; Marenich, A. V.; Bloino, J.; Janesko, B. G.; Gomperts, R.; Mennucci, B.; Hratchian, H. P.; Ortiz, J. V.; Izmaylov, A. F.; Sonnenberg, J. L.; Williams-Young, D.; Ding, F.; Lipparini, F.; Egidi, F.; Goings, J.; Peng, B.; Petrone, A.; Henderson, T.; Ranasinghe, D.; Zakrzewski, V. G.; Gao, J.; Rega, N.; Zheng, G.; Liang, W.; Hada, M.; Ehara, M.; Toyota, K.; Fukuda, R.; Hasegawa, J.; Ishida, M.; Nakajima, T.; Honda, Y.; Kitao, O.; Nakai, H.; Vreven, T.; Throssell, K.; Montgomery, J. A., Jr. ; Peralta, J. E.; Ogliaro, F.; Bearpark, M. J.; Heyd, J. J.; Brothers, E. N.; Kudin, K. N.; Staroverov, V. N.; Keith, T. A.; Kobayashi, R.; Normand, J.; Raghavachari, K.; Rendell, A. P.; Burant, J. C.; Iyengar, S. S.; Tomasi, J.; Cossi, M.; Millam, J. M.; Klene, M.; Adamo, C.; Cammi, R.; Ochterski, J. W.; Martin, R. L.; Morokuma, K.; Farkas, O.; Foresman, J. B.; Fox, D. J. *Gaussian 16 rev C.01*, Gaussian, Inc.: Wallingford, CT, USA, 2016.
[28] J.K.G. Watson, Determination of Centrifugal Distortion Coefficients of Asymmetric-Top Molecules, J. Chem. Phys. 46 (1967) 1935–1949, https://doi.org/10.1063/1.1840957.
[29] R.A. Motiyenko, L. Margulès, E.A. Alekseev, J.C. Guillemin, J. Demaison, Centrifugal Distortion Analysis of the Rotational Spectrum of Aziridine: Comparison of Different Hamiltonians, J. Mol. Spectrosc. 264 (2010) 94–99, https://doi.org/10.1016/j.jms.2010.09.007.
[30] G. Winnewisser, Millimeter Wave Rotational Spectrum of HSSH and DSSD. II. Anomalous K Doubling Caused by Centrifugal Distortion in DSSD, J. Chem. Phys. 56 (1972) 2944–2954, https://doi.org/10.1063/1.1677629.
[31] D.R. Jean, S.A. Wood, B.J. Esselman, R.C. Woods, R.J. McMahon, Rotational Spectroscopy of 1-Cyano-2-methylenecyclopropane (C_5H_5N)—A Newly Synthesized Pyridine Isomer, J. Phys. Chem. A 128 (2024) 1427–1437, https://doi.org/10.1021/acs.jpca.3c08002.
[32] P.M. Higgins, B.J. Esselman, M.A. Zdanovskaia, R.C. Woods, R.J. McMahon, Millimeter-wave spectroscopy of the chlorine isotopologues of chloropyrazine and twenty-two of their vibrationally excited states, J. Mol. Spectrosc. 364 (2019) 111179, https://doi.org/10.1016/j.jms.2019.111179.
[33] P.M. Dorman, B.J. Esselman, P.B. Changala, M.C. McCarthy, R.C. Woods, R. J. McMahon, Rotational spectra of twenty-one vibrational states of [^{35}Cl]-and [^{37}Cl]-chlorobenzene, J. Mol. Spectrosc. 394 (2023) 111776, https://doi.org/10.1016/j.jms.2023.111776.
[34] B.J. Esselman, M.A. Zdanovskaia, R.C. Woods, R.J. McMahon, Millimeter-wave spectroscopy of the chlorine isotopologues of 2-chloropyridine and twenty-three of their vibrationally excited states, J. Mol. Spectrosc. 365 (2019) 111206, https://doi.org/10.1016/j.jms.2019.111206.
[35] E.C. Fayolle, K.I. Öberg, J.K. Jørgensen, K. Altwegg, H. Calcutt, H.S.P. Müller, M. Rubin, M.H.D. van der Wiel, P. Bjerkeli, T.L. Bourke, A. Coutens, E.F. van Dishoeck, M.N. Drozdovskaya, R.T. Garrod, N.F.W. Ligterink, M.V. Persson, S. F. Wampfler, H. Balsiger, J.J. Berthelier, J. De Keyser, B. Fiethe, S.A. Fuselier, S. Gasc, T.I. Gombosi, T. Sémon, C.-Y. Tzou, Protostellar and cometary detections of organohalogens, Nat. Astron. 1 (2017) 703–708, https://doi.org/10.1038/s41550-017-0237-7.
[36] R. Navarro-González, E. Vargas, J. de la Rosa, A.C. Raga, C.P. McKay, Reanalysis of the Viking results suggests perchlorate and organics at midlatitudes on Mars, J. Geophys. Res. 115 (2010) E12010, https://doi.org/10.1029/2010JE003599.
[37] H.M. Pickett, R.L. Poynter, E.A. Cohen, M.L. Delitsky, J.C. Pearson, H.S.P. Müller, Submillimeter, millimeter, and microwave spectral line catalog, J. Quant. Spectrosc. Radiat. Transf. 60 (1998) 883–890, https://doi.org/10.1016/S0022-4073(98)00091-0.
[38] G. Herzberg, Molecular Spectra and Molecular Structure II, Infrared and Raman Spectra of Polyatomic Molecules, Van Nostrand Reinhold, New York, 1950.